ISSN 2616-5767 Vol.7, Issue 3: 54-63, DOI: 10.25236/AJETS.2024.070308

Design and Simulation of a High-Efficiency Cyclone Separator for Bioaerosol Collection

Jiao Ren, Weijie Liu, Yanni Zhang, Jinhua Liu[a,*], Zhanwu Ning

Institute of Urban Safety and Environmental Science, Beijing Academy of Science and Technology, Beijing, 100052, China
[a]afuliujh@163.com
[*]Corresponding author

Abstract: *In this paper, we utilized the computational fluid dynamics (CFD) method to develop models A1 to A6 with varying column-cone ratios for the wet-wall cyclone sampler. The results indicate that within the pressure drop range of (869.7, 997.8) Pa, model A4 (with a column-cone ratio of 1:2) exhibits the highest collection efficiency, surpassing the lowest by 6.7%. In addition, we modeled B1-B3 with different cyclone heights and found that a cyclone height of 50 mm was most effective for balancing cyclone structures and improving collection efficiency.*

Keywords: *Bioaerosol Sampling, Wet-Wall Cyclone Field, Efficient Collection, Geometric Parameters*

1. Introduction

Bioaerosol is dispersion system in which solid or liquid particles containing biological components are suspended in a gaseous medium[1]. Various biological aerosol particles, such as bacteria, fungal spores, viruses, archaea, pollen, algae and other biological fragments[2,3] (e.g., endotoxins, glucans, etc.), are scattered in the atmosphere. These particles typically range in size from 1 nm to 100 μm[3]. These bioactive particles can enter the body through various ways[4]. Pathogenic and allergenic aerosol particles pose a substantial threat to public health[5-7].

Quantifying the concentration of bioaerosol particles is an essential task in health assessment, which creates a significant demand for the collection and analysis of these particles. Airborne environments, however, have an extremely low density of biological material[8,9], making sampling work difficult. In addition, the small size of microbial particles is another major challenge for sampling[9]. The trapping effect of biological aerosols directly impacts the subsequent analysis, meaning that different sampling methods can greatly affect evaluation results. Therefore, the sampling technology of wet-wall cyclone has been developed to ensure the biological activity of particles and improve the capture rate[10,11]. Sung et al.[12]developed an online virus detection system with a horizontal wet-cyclone sampler as the core component, and verified its operation through quantitative experiments on virus concentration in the air. Hubbard et al.[13] established the critical film evaporation model for the horizontal wet-cyclone sampler. By using optimized model parameters, the calculation accuracy of liquid evaporation rate in the full range of relative humidity and temperature is improved. King et al[14] compared the cell culturability and DNA integrity of Escherichia coli collected by the wet-wall cyclone and the inertial impactor. it was shown that wet-wall cyclone sampling is gentler and can better preserve the biological activity of Escherichia coli by analyzing the results of classical microbiological plating techniques, pulsed-field gel electrophoresis, and real-time polymerase chain reaction. Cho et al.[15]optimized the liquid film formed in the real wetted wall cyclone, and determined the optimal flow conditions of gas and liquid to create a stable film using numerical analysis. Heo et al.[10]summarized the effects of silica nanoparticle concentration and heat-treatment temperature on the water contact angle, and prepared a super-hydrophilic wall coating material. The transfer rate of aerosol-to-hydrosol was demonstrated to be approximately 95.9% at the particle size of 500 nm by using this material.

We optimized two important geometric parameters, namely cyclone height (H) and cylinder-to-cone ratio (h/Lc), and idebtified the key structural factors that affect particle behavior in the flow field through three-dimensional CFD simulation.

ISSN 2616-5767 Vol.7, Issue 3: 54-63, DOI: 10.25236/AJETS.2024.070308

2. Description of the sampling principle

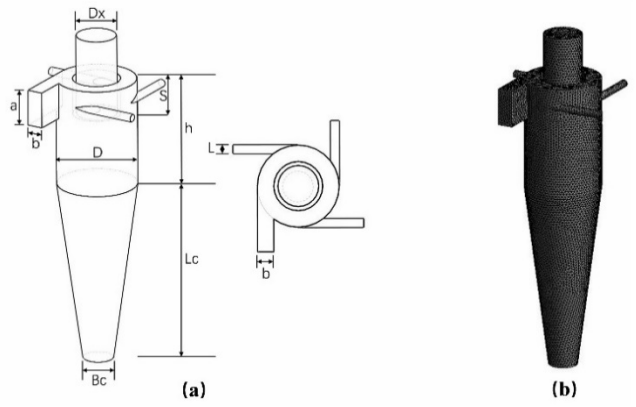

Figure 1: Configuration (a) and grid (b) representation of the wet-cyclone sampler

Table 1: Parameters and symbols of the wetted wall cyclone

Parameter	Symbol
Body diameter	D
Gas inlet height	a
Gas inlet width	b
Gas outlet diameter	Dx
Liquid inlet diameter	L
Liquid outlet diameter	Bc
Vortex finder length	S
Cylinder height	h
Cone height	Lc
Cyclone height	H

The wet-cyclone sampler is an inertial separator driven by centrifugal force. It is mainly composed of cyclone body, vortex finder, inlet and exit parts (Fig. 1(a)). Among them, cyclone body is the main part of separation, which consists of a cylindrical body and a conical part with the fixed diameter. The specific structure description of the sampler is shown in Table 1. The motion of bioaerosol particles in the sampler can be described as follows: The particulate-laden air flows into the sampler through the tangential inlet[16]. This steers the sampled air to spin rapidly inside the sampler and spiral downward towards the conical section of the cyclone (outer vortex). Under the influence of centrifugal and shear forces generated by the high-speed rotating airflow, a stable liquid film forms on the inner wall of the cyclone separator (see Fig. 2, where the blue portion indicates the liquid film). The microbial particles that enter the cyclone with the air are pushed towards the wet wall by the internal helical air stream and flow along with the sampling liquid to be collected at the underflow[16]. As the cone contracts, the rotating airflow develops inward and upward (forming an inner vortex). The inner vortex, carrying particles that were not captured, is discharged through the upper outlet of the cyclone (Fig. 2) [17].

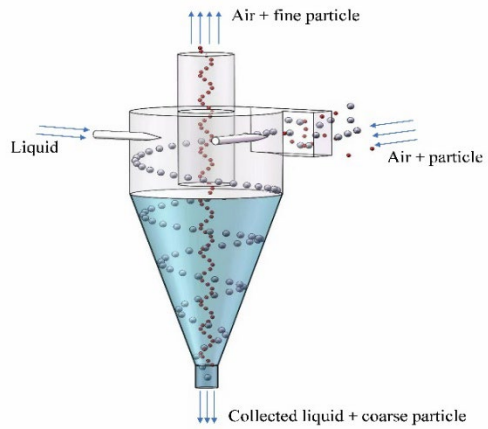

Figure 2: Sampling schematic diagram of the wet-cyclone separator

ISSN 2616-5767 Vol.7, Issue 3: 54-63, DOI: 10.25236/AJETS.2024.070308

3. Mathematical modeling

3.1 Model description

3.1.1 Flow field

To avoid the complexity of fluid molecular motion and focus on the macroscopic motion of fluid, the equilibrium and motion laws of fluid can be studied using analytic method. The collected air is considered to be a continuous medium consisting of numerous fluid particles that are continuously distributed. And the calculation of this continuous phase can be completed by solving the flow field control equation. The turbulent flow is properly simplified by using the ensemble averaging method, resulting in the derivation of the Reynolds time-averaged Navier-Stokes equation (RANS) for incompressible fluid flow[18]:

$$\frac{\partial \overline{u_i}}{\partial t}+\overline{u_j}\frac{\partial \overline{u_i}}{\partial x_j}=f_i-\frac{1}{\rho}\frac{\partial \overline{P}}{\partial x_i}+\frac{1}{\rho}\frac{\partial}{\partial x_j}\left(\mu\frac{\partial \overline{u_i}}{\partial x_j}-\rho\overline{u_i'u_j'}\right) \tag{1}$$

where, the superscripts $i,j=1,2,3$ represent the components of the Cartesian coordinate system, u, ρ, and μ is the velocity, density, and dynamic viscosity of the fluid, respectively. P is the pressure, x is the position, f is the force per unit mass, and t is the time for fluid flow. $-\rho\overline{u_i'u_j'}$ is defined as the Reynolds stress tensor, which indicates the effects of turbulent fluctuations on fluid flow. The overbar represents the Reynolds-averaged terms.

To achieve mathematical closure of the equations, it is necessary to incorporate a turbulence model as an additional condition to account for the Reynolds stress term. The key to selecting a turbulence model is accurately describing the pulsation of the entire flow field. The anisotropy of airflow, is highly evident in this study, and this characteristic will also be a crucial factor to consider when selecting a turbulence model. The Reynolds stress model has been proven to be the most accurate model for describing the strongly swirling flows found in cyclones[19-21]. However, it is difficult to achieve convergence in the calculation[21], and it is also more computationally expensive[22]. Therefore, the RNG k-ε turbulence model is employed to supplement the Reynolds-averaged Navier-Stokes equation (RANS). Furthermore, our model also takes into account the rotation effect, which improves the calculation accuracy of strong swirling flow.

Since the air stream in a swirling cyclone and the resulting liquid film move similarly, equations (1) can be considered true for both[23].

In the wet-wall cyclone field, two continuous phases, air and sampling liquid, coexist in the same space and penetrate each other. To accurately represent the distribution of gas-liquid flows, we utilize the Eulerian multiphase model to solve for each phase. At present, we have successfully established the mathematical model of the flow field of the wet wall cyclone.

3.1.2 Particle trajectory

Based on the force balance theory[18], the momentum equation of a single particle can be expressed as:

$$\frac{du_{p,i}}{dt}=\left(\frac{18\mu_{air}}{\rho_p d_p^2}\right)\left(\frac{C_D\,\mathrm{Re}_p}{24}\right)\left(u_{air,i}-u_{p,i}\right)+\left(\frac{\rho_p-\rho_{air}}{\rho_p}\right)g_i+F_i \tag{2}$$

Here, the superscript i represents the components of the Cartesian coordinate system; u_{air}, ρ_{air} and μ_{air} is the velocity, density and dynamic viscosity of the gas respectively; u_p, d_p and ρ_p is the velocity, diameter , and density of the particles respectively; t is the movement time of the particles; g is gravity acceleration; C_D is the drag coefficient; F is the additional force per unit mass of particles; and particle relative Reynolds number (Re_p) is defined as:

ISSN 2616-5767 Vol.7, Issue 3: 54-63, DOI: 10.25236/AJETS.2024.070308

$$\mathrm{Re}_p = \frac{\rho_{air} d_p \left| u_p - u_{air} \right|}{\mu_{air}} \tag{3}$$

3.2 Numerical simulations

3.2.1 Cyclone design

In order to evaluate the significance of cyclone geometric dimensions on collection performance characteristics and develop a miniature cyclone capable of collecting microbial aerosol particles, we modified two aspects of the cyclone modified using Stairmand's design (refer to cyclone A3). These modifications included adjusting the cyclone height and cylinder-to-cone ratio. Several cyclone separators with different sizes were designed, as detailed in Table 2.

Table 2: Geometric dimensions of experimental cyclones

Wet-cyclone models	Geometry	Dimension	length(mm)
	D	1.0D	10
	a	0.5D	5
	b	0.2D	2
	L	0.1D	1
	S	0.5D	5
	B_C	0.375D	3.75
A1	h/Lc[c]	1.5/1.5	20/20
A2		1.5/2.0	17/23
A3[a]		1.5/2.5	15/25
A4[b]		1.5/3.0	13/27
A5		1.5/3.5	12/28
A6		1.5/4.0	11/29
B1[b]	H	4D	40
B2		5D	50
B3		6D	60

[a] Stairmand's high efficiency cyclone model (standard cyclone model)
[b] Cyclone A4 and B1 are identical
[c] Cylinder-to-cone ratio

3.2.2 Simulation conditions

The construction of the wet-wall cyclone separator model studied in this paper is complicated. Therefore, in order to ensure the stability and convergence of the subsequent calculation, we adopted the patch conformal algorithm and the unstructured tetrahedral mesh, and we also encrypted the parts with high velocity locally (Fig. 1(b)).

In the simulation, the air inlet and liquid inlet serve as the velocity-inlet boundary conditions. The air supply is set at 16 L/min and the liquid supply is set at 9 mL/h. The air outlet functions could be seen as a pressure-outlet, allowing particles to escape, while the liquid outlet is a stationary wall that can trap particles. The wall surface of the cyclone separator can be categorized into two types: the area with the liquid film is considered the wall with trapping ability, while the rest is designated as the wall with complete reflection property. We chosed liquid water as the working fluid, and the surface tension coefficient of water in air is 0.072 N/m in this article. By changing the parameter Settings, the particles enter the separator as a discrete phase with air through the normal direction of the air intake. And the injection speed of the particles is equal to the inlet speed of the air. The concentration of the particles is 100 particles/cm3 air, and its density is 1060 kg/m3.

In this paper, we used RNG k-ε turbulence model and Euler polyphase model. The standard wall function is applied. The SIMPLE algorithm is employed for performing the pressure-velocity coupling, the central difference method is used to disperse the diffusion phase, and the second-order upwind scheme is utilized for spatial discretization.

ISSN 2616-5767 Vol.7, Issue 3: 54-63, DOI: 10.25236/AJETS.2024.070308

4. Results and discussion

4.1 Simulation of wet-wall cyclone field

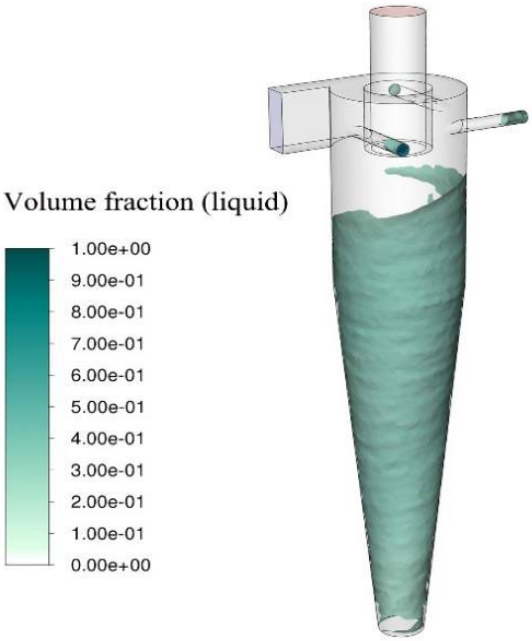

Figure 3: Illustration of volume fraction for the sampling liquid

We used the Euler multiphase model to simulate the wet wall cyclone in the flow field at the inlet velocity of 16 L/min and 9 mL/h. Centrifugal force and shear force generated by high air velocity form a stable liquid film on the inner wall of the cyclone separator (Fig. 3). Through simulating, the distribution of the liquid phase in the wet-wall cyclone field is displayed intuitively, confirming the presence of a liquid film adhering to the wall.

4.2 Effects of geometrical factors on the performance of wet-wall cyclone separators

The air swirls as a vortex, and the gas stream constitutes a double vortex in the cyclone: the outer one is the free vortex rotation, flowing helically down in the near-wall area; the inner one is the forced vortex rotation, spiraling towards the exit of the vortex finder, which creates a pressure cavity at the center of the swirling flow, where the pressure difference could be zero or even negative compared to the ambient (Fig. 4).

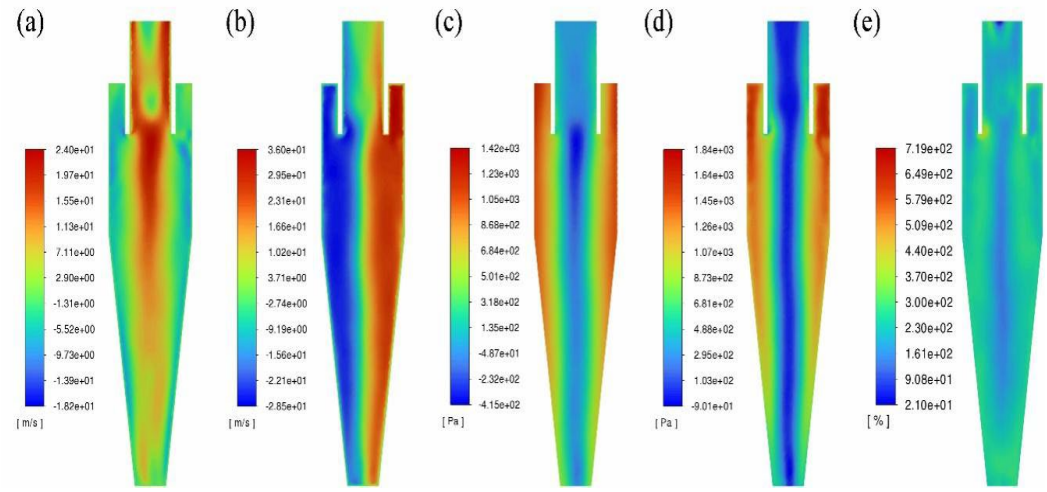

Figure 4: Contour plots of (a) axial velocity (b) tangential velocity (c) static pressure (d) total pressure (e) turbulent intensity of standard cyclone model

ISSN 2616-5767 Vol.7, Issue 3: 54-63, DOI: 10.25236/AJETS.2024.070308

4.2.1 Effect of cylinder-to-cone ratios

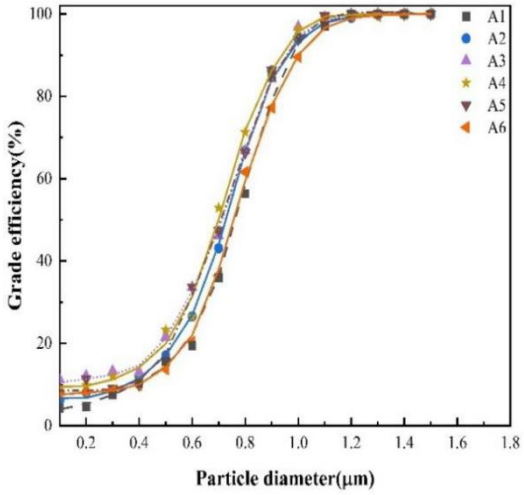

Figure 5: Grade efficiency curves for cyclone models A1-A6 at Uin=26.7 m/s

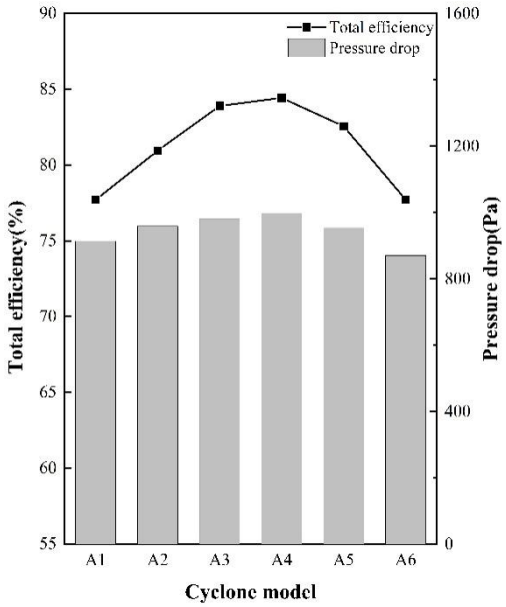

Figure 6: The effect of decreasing the cylinder-to-cone ratio on (a) total collection efficiency, and (b) the pressure drops.

To investigate the influence of the column-cone ratio of a wet-wall cyclone on its performance, including particle collection efficiency and pressure drop, six different models of cyclone separators (A1, A2, A3, A4, A5, and A6) listed in Table 2 were selected for the CFD numerical simulation study. The body diameter (Dx) is 10 mm, cyclone height(H) is 40 mm, the diameter of the air outlet is 5 mm, the air supply speed is 16 L/min, and the water supply speed is 9 mL/h in this simultiion study.

From cyclone model A1 to cyclone model A6, whose total collection efficiency increases and then decreases with the decreasing cylinder-cone ratio of the model. Among these models, A3, A4, and A5 have the highest total collection efficiency for particles ranging from 0.1 to 1.5 μm, which are 83.9%, 84.4%, and 82.6%, respectively, with A4 being particularly noteworthy (Fig. 5,Fig. 6). The pressure drop in the cyclone separator follows the same trend. The pressure drop indicates the energy required by the device for collection purposes and can be regarded as the static pressure difference between the inlet and outlet. In practice, it is always desired to have the smaller pressure drop and the higher collection efficiency at the same time. Within the specific range of column-to-cone ratio, the pressure drops range from 869.7 Pa to 997.8 Pa in type A cyclones,the maximum pressure drop is 14.7% higher than the minimum, and the total collection efficiency increases by 6.7%.

ISSN 2616-5767 Vol.7, Issue 3: 54-63, DOI: 10.25236/AJETS.2024.070308

The evaluation of collection efficiency is mainly based on two factors: separation performance and capture performance. According to the analysis in section 2.1 of this paper, the separation effect is determined by the resultant force (F˙). The total height of cyclone model A remains constant, while the rotating diameter (D') of the outer cyclone can be adjusted by changing the ratio of the cylinder to the cone, which can be demonstrated by comparing the inner diameter of samplers at the axial position y = H/2 (Fig. 7). The decrease in the airflow's rotating diameter from A1 to A4 leads to an increase in centrifugal force, which benefits particle separation. Similarly, the separation effect is further enhanced from model A4 to model A6 for the same reason. However, the effective area (liquid film area) for trapping particles is decreasing at a rate of approximately 2.4%, which hampers its ability to capture particles,as detailed in Figure 8.

Therefore, in models A1 to A6, as the inner diameter of the outer vortex decreases, the separation performance gradually is improved, while the trapping performance is weaken due to the reduction in effective trapping area. In models A1 to A4, the increase in separation performance dominates in the resulting in a gradual increase in collection efficiency. In models of A4 to A6, the weakening capture performance leads to a gradual decrease in collection efficiency. Therefore, when the column-cone ratio of the model is 1:2 (cyclone model A4), the wet-wall cyclone sampler achieves the highest collection efficiency.

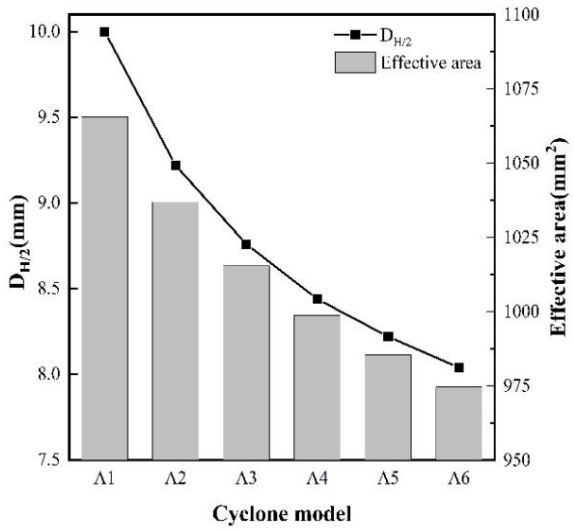

Figure 7: (a) Inner diameter at Y=H/2, (b) the effective area for particle capture in cyclone models A1-A6

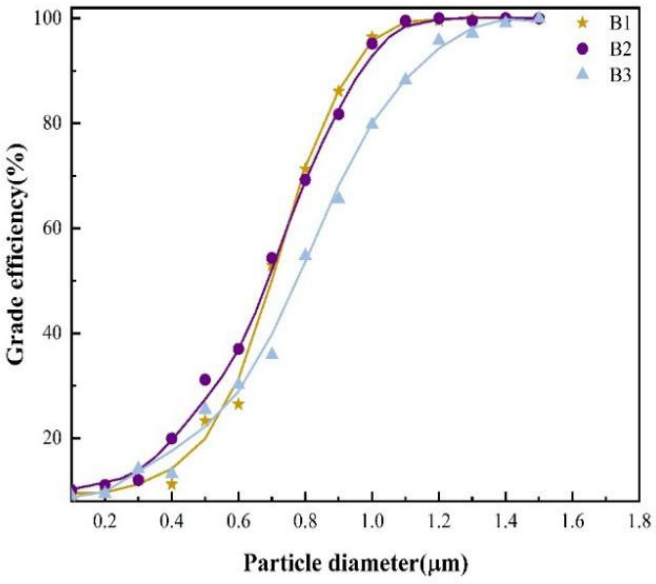

Figure 8: Grade efficiency curves for cyclone models B1-B3 at Uin=26.7 m/s

ISSN 2616-5767 Vol.7, Issue 3: 54-63, DOI: 10.25236/AJETS.2024.070308

4.2.2 Effect of the cyclone height

Table 3: Total collection efficiency for the wetted wall cyclones with different cyclone heights

Cyclone models	Cyclone height (mm)	Total efficiency (%)
B1	40	84.4
B2	50	86.0
B3	60	76.9

The CFD numerical simulation was conducted on cyclone separators (models B1, B2, and B3) with body diameter (D) of 10 mm, column-cone ratio of 1:2, vortex finder diameter (Dx) of 5 mm, and three different cyclone heights (40mm, 50mm, and 60mm). We analyzed the influence of cyclone height on the collection efficiency of sampler in this study,as detailed in Table 3.

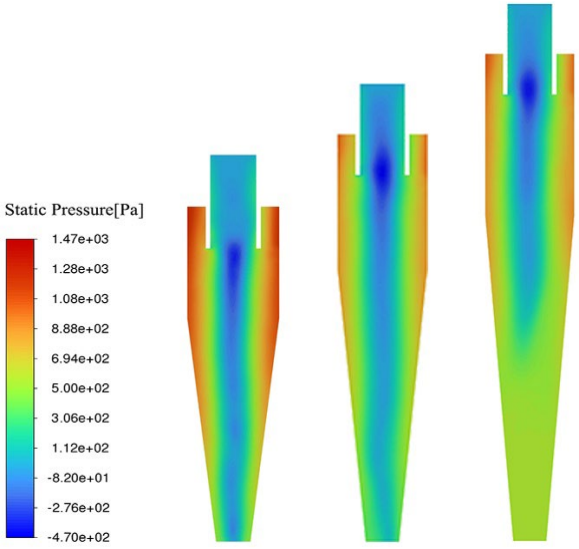

Figure 9: Color map of static pressure distribution in cyclones at different heights of the cyclone.

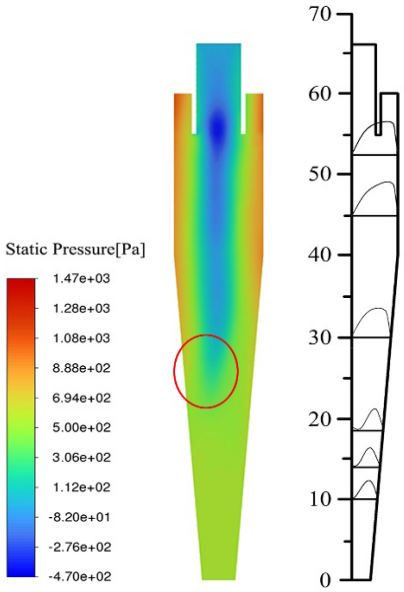

Figure 10: Tangential velocity profiles at different axial sections for cyclone B3. The red circle indicates the position of the vortex end.

The collection efficiency of cyclone B2 is 1.6% higher than that of B1 for collecting particles with the diameter of 0.1 to 1.5 μm, while the collection efficiency of cyclone B3 is 9.1% lower than that of B2. This indicates that the cyclone height has a significant impact on the collection efficiency. When all other conditions remain unchanged, increasing the cyclone height initially leads to an increase in the collection efficiency, followed by an obvious decrease,as detailed in Figure 9.

The simulation results indicate that there is a critical value for the cyclone height. Once the cyclone

ISSN 2616-5767 Vol.7, Issue 3: 54-63, DOI: 10.25236/AJETS.2024.070308

height surpasses this threshold, the performance conspicuously deteriorates. This critical value is the natural vortex length. When the cyclone height of the separator exceeds the natural vortex length, the vortex end deflects and will collide with the wall (Fig. 10). The maximum tangential velocity of the airflow above the vortex end is greater than 21.4 m/s, while the maximum tangential velocity below the vortex end rapidly decreases to below 3.6 m/s, leading to a sharp decrease in centrifugal force. This proves that the separation performance of the region below the vortex end is much worse compared to that above. Furthermore, the deviation of the inner vortex leads to vortex oscillation and the re-entrainment of previously captured particles, ultimately resulting in a reduction in collection efficiency, which could be the primary reason for the degradation in performance of cyclone model B3. However, when the cyclone height is less than the natural vortex length, meaning that the vortex end does not appear in the cyclone body. Increasing the cyclone height will enhance the space available for separation and capture. In this situation, the collection efficiency will improve as the cyclone height increases.

To sum up, the design of a wet-wall cyclone separator should take into account the vortex turning. Here, we utilized numerical simulation to determine the optimal height for the cyclone model, and found that 50 mm is the most effective cyclone height for balancing the vortex structure and enhancing collection efficiency.

5. Conclusions and outlook

In this paper, CFD simulation is utilized to study the influence of key geometric parameters (column-cone ratio and cyclone height) on the collection efficiency of the wet-wall cyclone sampler. The main findings are as follows:

(1) As the ratio of column to cone decreases, the collection efficiency initially increases and then decreases. The optimal ratio for the cyclone models is 1:2. When the ratio of column to cone is greater than 1:2, the main factor affecting the collection efficiency of the wet-wall cyclone sampler is the separation performance determined by centrifugal force and drag force. Conversely, when the ratio of column to cone is less than 1:2, the primary factor that influences the collection efficiency is the trapping performance.

(2) With the increase in cyclone height, the inner vortex deflects towards the wall, and the vortex end reaches the cone of the separator, causing particles re-entrainment. This results in a noticeable reduction in collection efficiency. We determined that the optimal cyclone height is 50 mm through numerical simulation in this study.

Through theoretical analysis and numerical calculations, some optimization suggestions were put forward for the design of a wet separation sampler to improve the collection efficiency of micron and submicron particles. However, the design and implementation of the aerosol sampling process, with the wet-wall cyclone separator as the core, involves numerous theories, methods, and technologies, needs further research and development. This includes considering the fragmentation and agglomeration of aerosol particles, the formation of atomized particles, etc. Additionally, the selection of sampling liquid and the flow ratio of injected gas and liquid should be optimized, too.

Acknowledgements

This research was supported by the National Natural Science Foundation of China (22178022) and the Science and Technology Initiation Program of the Beijing Academy of Science and Technology (AH-RCB-230418).

References

[1] X. Z. Ma, Z. Q. Fang, F. S. Li, K. X. Hu, Determination of performance-parameter design and impact factors of sampling efficiency for bioaerosol cyclones. Biotechnol. Biotechnol. Equip. 34, 640-651 (2020).
[2] W. Hu et al., Biological Aerosol Particles in Polluted Regions. Curr. Pollut. Rep. 6, 65-89 (2020).
[3] V. R. Després et al., Primary biological aerosol particles in the atmosphere: a review. Tellus Ser. B-Chem. Phys. Meteorol. 64, 58 (2012).
[4] H. T. Gao et al., Atmospheric-pressure non-equilibrium plasmas for effective abatement of pathogenic biological aerosols. Plasma Sources Sci. Technol. 30, 17 (2021).
[5] S. D. Judson, V. J. Munster, Nosocomial Transmission of Emerging Viruses via Aerosol-Generating

ISSN 2616-5767 Vol.7, Issue 3: 54-63, DOI: 10.25236/AJETS.2024.070308

Medical Procedures. Viruses-Basel 11, 12 (2019).
[6] P. E. Taylor, R. C. Flagan, R. Valenta, M. M. Glovsky, Release of allergens as respirable aerosols: A link between grass pollen and asthma. J. Allergy Clin. Immunol. 109, 51-56 (2002).
[7] M. Shiraiwa et al., Aerosol Health Effects from Molecular to Global Scales. Environ. Sci. Technol. 51, 13545-13567 (2017).
[8] S. Yooseph et al., A Metagenomic Framework for the Study of Airborne Microbial Communities. PLoS One 8, 13 (2013).
[9] X. Y. Li et al., A Robot Assisted High-flow Portable Cyclone Sampler for Bacterial and SARS-CoV-2 Aerosols. Aerosol Air Qual. Res. 21, 13 (2021).
[10] K. J. Heo, H. S. Ko, S. B. Jeong, S. B. Kim, J. H. Jung, Enriched Aerosol-to-Hydrosol Transfer for Rapid and Continuous Monitoring of Bioaerosols. Nano Lett. 21, 1017-1024 (2021).
[11] Y. S. Cho et al., Continuous Surveillance of Bioaerosols On-Site Using an Automated Bioaerosol-Monitoring System. ACS Sens. 5, 395-403 (2020).
[12] G. Sung, C. Ahn, A. Kulkarni, W. G. Shin, T. Kim, Highly efficient in-line wet cyclone air sampler for airborne virus detection. J. Mech. Sci. Technol. 31, 4363-4369 (2017).
[13] J. A. Hubbard, O. A. Ezekoye, J. S. Haglund, Modeling Liquid Film Evaporation in a Wetted Wall Bioaerosol Sampling Cyclone. J. Therm. Sci. Eng. Appl. 5, 10 (2013).
[14] M. D. King, A. R. McFarland, Bioaerosol Sampling with a Wetted Wall Cyclone: Cell Culturability and DNA Integrity of Escherichia coli Bacteria. Aerosol Sci. Technol. 46, 82-93 (2012).
[15] Y. S. Cho, S. C. Hong, J. Choi, J. H. Jung, Development of an automated wet-cyclone system for rapid, continuous and enriched bioaerosol sampling and its application to real-time detection. Sens. Actuator B-Chem. 284, 525-533 (2019).
[16] K. Pant, C. T. Crowe, P. Irving, On the design of miniature cyclones for the collection of bioaerosols. Powder Technol. 125, 260-265 (2002).
[17] D. Park, J. S. Go, Design of Cyclone Separator Critical Diameter Model Based on Machine Learning and CFD. Processes 8, 13 (2020).
[18] R. A. F. Oliveira, V. G. Guerra, G. C. Lopes, Improvement of collection efficiency in a cyclone separator using water nozzles: A numerical study. Chem. Eng. Process. 145, 13 (2019).
[19] K. Elsayed, C. Lacor, Optimization of the cyclone separator geometry for minimum pressure drop using mathematical models and CFD simulations. Chem. Eng. Sci. 65, 6048-6058 (2010).
[20] T. G. Chuah, J. Gimbun, T. S. Y. Choong, A CFD study of the effect of cone dimensions on sampling aerocyclones performance and hydrodynamics. Powder Technol. 162, 126-132 (2006).
[21] J. Gimbun, T. G. Chuah, T. S. Y. Choong, A. Fakhru'l-Razi, A CFD Study on the Prediction of Cyclone Collection Efficiency. International Journal for Computational Methods in Engineering Science and Mechanics Vol.6, 161-168 (2005).
[22] Y. J. Xiao et al., Optimal design of a wet-type desulphurization absorber by the numerical simulation method. Chem. Eng. Res. Des. 92, 1257-1266 (2014).
[23] G. I. Sigaev et al., Development of a cyclone-based aerosol sampler with recirculating liquid film: Theory and experiment. Aerosol Sci. Technol. 40, 293-308 (2006).